Adaptive potentiation in rod photoreceptors after light exposure

Alex S. McKeown and Timothy W. Kraft

Department of Vision Sciences, University of Alabama at Birmingham, Birmingham, AL 35294

Photoreceptors adapt to changes in illumination by altering transduction kinetics and sensitivity, thereby extending their working range. We describe a previously unknown form of rod photoreceptor adaptation in wild-type (WT) mice that manifests as a potentiation of the light response after periods of conditioning light exposure. We characterize the stimulus conditions that evoke this graded hypersensitivity and examine the molecular mechanisms of adaptation underlying the phenomenon. After exposure to periods of saturating illumination, rods show a 10–35% increase in circulating dark current, an adaptive potentiation (AP) to light exposure. This potentiation grows as exposure to light is extended up to 3 min and decreases with longer exposures. Cells return to their initial dark-adapted sensitivity with a time constant of recovery of $\sim$7 s. Halving the extracellular Mg concentration prolongs the adaptation, increasing the time constant of recovery to 13.3 s, but does not affect the magnitude of potentiation. In rods lacking guanylate cyclase activating proteins 1 and 2 (GCAP$^{-/-}$), AP is more than doubled compared with WT rods, and halving the extracellular Mg concentration does not affect the recovery time constant. Rods from a mouse expressing cyclic nucleotide–gated channels incapable of binding calmodulin also showed a marked increase in the amplitude of AP. Application of an insulin-like growth factor-1 receptor (IGF-1R) kinase inhibitor (Tyrphostin AG1024) blocked AP, whereas application of an insulin receptor kinase inhibitor (HNMPA(AM)$_3$) failed to do so. A broad-acting tyrosine phosphatase inhibitor (orthovanadate) also blocked AP. Our findings identify a unique form of adaptation in photoreceptors, so that they show transient hypersensitivity to light, and are consistent with a model in which light history, acting via the IGF-1R, can increase the sensitivity of rod photoreceptors, whereas the photocurrent overshoot is regulated by Ca-calmodulin and Ca^{2+}/Mg^{2+}-sensitive GCAPs.

INTRODUCTION

Adaptation in the visual system is essential for maintaining perception across a large range of light levels. Two principle features of photoreceptor light adaptation are decreased sensitivity to light and accelerated response recovery (Tamura et al., 1991; Woodruff et al., 2008). Mutations have been identified that constrict the adaptive ranges of rods and cones, and most of these mutations have been mapped to loss of protein function (Gal et al., 1994; Jiang and Baehr, 2010; Naeem et al., 2012). Transgenic mouse models have demonstrated how alteration or loss of phototransduction proteins can limit cellular adaptation. Mouse rods lacking guanylate cyclase activating proteins 1 and 2 (GCAP$^{-/-}$) or regulator of G-protein signaling (RGS) proteins exhibit dramatically slower response recovery and have diminished adaptive capabilities (Chen et al., 2000; Burns et al., 2002; Krispel et al., 2006; Dizhoor et al., 2010). More subtle changes in rod light adaptation occur as the result of phosphorylation of phosphodiesterase 6 (PDE6), where mutation of tyrosine residues on the PDE6-γ subunit eliminates recovery acceleration (Woodruff et al., 2008). Although many features and components have been discovered,

the current model of photoreceptor adaptation is incomplete. Here we present a paradoxical form of adaptation in which WT rods become more sensitive after light exposure.

The recovery rate of a saturated light response, the speed of reopening of CNG channels, is strongly dependent on Mg^{2+} ions, as GCAPs require both Ca^{2+} and Mg^{2+} to regulate guanylate cyclase activity and terminate the light response (Dizhoor et al., 2010; Azevedo and Rieke, 2011). We show that Mg^{2+} concentration affects the duration of our newly described adaptive potentiation (AP) but not its magnitude. We also attribute the Mg^{2+} dependence of the adaptation to GCAPs, as animals lacking both GCAPs had recovery rates independent of Mg^{2+} concentration. Another cation-dependent protein, calmodulin, interacts with the CNG channels and modulates channel sensitivity for cGMP (Bauer, 1996). However, rods incapable of binding calmodulin exhibit features of classical light adaptation (Chen et al., 2010). Here we demonstrate that calmodulin is partially responsible for attenuating large fluctuations in circulating current during recovery from saturating illumination.

Correspondence to Timothy W. Kraft: twkraft@uab.edu

Abbreviations used in this paper: AP, adaptive potentiation; ERG, electroretinogram; GCAP, guanylate cyclase activating protein; IGF-1R, insulin-like growth factor-1 receptor; IR, insulin receptor.

The phosphorylation state of the CNG channel α subunit modulates the sensitivity of the receptor, but there is inconclusive evidence supporting a role for channel phosphorylation in light adaptation (Gordon et al., 1992; Molokanova et al., 1997). The insulin-like growth factor-1 receptor (IGF-1R) and the insulin receptor (IR) are both expressed in mammalian outer segments (Waldbillig et al., 1987; Zick et al., 1987) and may mediate opposing pathways that control the phosphorylation state of the channel. On one hand, strong activation of rhodopsin in a retinal explant stimulates IR kinase activity, resulting in phosphorylation of the CNG channel and reduced channel sensitivity (Rajala and Anderson, 2003; Gupta et al., 2012). On the other hand, recordings from single rods and isolated retina show that stimulation of the IGF-1R with its native ligand, IGF-1, increases response amplitude and cell sensitivity through an intermediate phosphatase, possibly protein tyrosine phosphatase-1B, that dephosphorylates the CNG channel (Savchenko et al., 2001). Here we demonstrate a similar increase in photoreceptor sensitivity elicited not by application of IGF-1, but by light exposure. We investigate the complex interaction of how GCAPs, calmodulin, and the IGF-1R and IR pathways contribute to rod photoreceptor sensitivity after saturating illumination. Just as PDE and guanylate cyclase oppose one another in regulating cGMP concentration, evidence is mounting that the IGF1R and IR may play analogous roles modulating the sensitivity of the CNG channel for its ligand, thus adding another layer of regulation of photoreceptor sensitivity.

MATERIALS AND METHODS

Animals

All experiments were performed in accordance with the Institutional Animal Care and Use Committee guidelines at the University of Alabama at Birmingham (UAB) under an approved animal protocol. The calmodulin mutant mice (CaMΔ) and GCAP knockout mice (GCAP$^{-/-}$) were obtained as a gift from the laboratory of J. Chen at the University of Southern California (USC; Los Angeles, CA). The mice were transferred under a material transfer agreement between UAB and USC. The WT, CaMΔ, and GCAP$^{-/-}$ mice were created on a C57BL/6J background and were maintained in animal care facilities under a normal 12-h light/dark cycle. Mice of either sex, between 1 and 6 mo of age, were used for all experiments. Details regarding the creation of the CaMΔ mouse line and the GCAP$^{-/-}$ mouse line can be accessed in Chen et al. (2010) and Mendez et al. (2001), respectively.

Single cell recordings

Mice were dark-adapted overnight before being sacrificed, and their eyes were enucleated under infrared illumination. The retinas were isolated into cold L-15 medium (Leibovitz, powder with glutamine; Sigma-Aldrich) under a dissection microscope (MS-5; Leica). Individual retinas were then chopped into ~0.1-mm^2 sections and transferred to the recording chamber. Cell viability was preserved using a perfusion solution of Locke's media that contained (mM): 120 NaCl, 3.6 KCl, 2.4 MgCl$_2$, 1.2 CaCl$_2$, 3 HEPES, 20 NaHCO$_3$, 0.02 EDTA, and 10 glucose. The perfusion solution was

kept between 36 and 37°C, and a gas mixture of O$_2$/CO$_2$ was adjusted to balance pH at 7.4. Single cells were drawn into glass microelectrodes with inner diameters of ~1.3 μm that were filled with a buffer solution similar to the medium above but lacking NaHCO$_3$, which was replaced with an additional 20 mM NaCl. Light stimuli were delivered via a two-channel optical bench focused at the specimen plane, with one channel delivering the short (2 ms) test stimuli and the second channel delivering the 20–300-s adapting stimuli. Stimuli from both channels were controlled by computer-driven Uniblitz shutters (Vincent Associates). The light sources for each channel were 100-W tungsten bulbs (Xenophot HLX 64623; Osram) powered by constant power sources (ATE 15-15M; Kepco Power Supplies). Stimulus intensity was controlled by calibrated neutral density filters, and stimulus wavelength was 500 nm (±5 nm, narrow band filter). Photocurrents were amplified using an Axopatch A-1 amplifier (Molecular Devices), low-pass filtered (200 Hz, 8-pole Bessel), and digitized at 1 KHz. Single cell responses were low-pass filtered post hoc at 30 Hz, 8-pole Bessel. All data were collected using custom LabView software (National Instruments). Offline analysis and filtering were performed using IGOR software (WaveMetrics).

Photon capture

The single photon response amplitude was calculated for individual cells using the ratio of the signal variance to the mean response for a large number of trials at or near threshold (Baylor et al., 1979). Dividing the mean response by the single photon response gave the mean number of activated rhodopsin molecules for those trials. The collecting area was calculated by dividing the number of activated rhodopsin molecules by the incident photons, as measured using a photometer (model 350 linear/log optometer; Graseby Optronics). Conditioning light intensities bleached at most 0.1% of the total rhodopsin in the cell, assuming 7.0×10^7 molecules of rhodopsin/rod (Breton et al., 1994; Lyubarsky et al., 2004). The mean adapting light exposure activated 230 ± 13 photoisomerizations per second (R*/s). Light stimuli below saturation (<90 R*/s) and light stimuli that produced significant bleach (>1,000 R*/s) were unreliable in eliciting AP.

Isolated retina electroretinography

Whole dark-adapted retinas were isolated in HEPES-buffered Locke's solution, as described in the single cell methods, with 10 mM BaCl$_2$ added to suppress the Müller cell (slow PIII) component of the electroretinogram (ERG) waveform (Karwoski et al., 1989). The retina was placed on a grease ring, photoreceptor side up, and was held in place by a circular piece of filter paper with a 2-mm diameter hole in the center. The preparation was then transferred to the recording apparatus, where the chamber was perfused with a 37°C solution of Locke's buffer. The perfusion solution also contained 10 mM D/L-aspartate and 25 μM (±)-2-amino-4-phosphonobutyric acid (AP-4; Sigma-Aldrich), a selective blocker of glutamic acid receptors found on the ON-bipolar cells (mGluR$_6$). Both the aspartate (by saturation) and the AP-4 (by selective inhibition) were used to block photoreceptor ON-bipolar cell synaptic transmission, thus isolating the photoreceptor response for analysis. Flow rate was set at 1.5 ml/min. The perfusion solution was bubbled with a 95/5% mixture of O$_2$/CO$_2$ to maintain pH at 7.4. Based on an end-on collecting area of 0.37 μm^2 for the mouse rod (Lyubarsky et al., 2004), the half-maximal intensity ($I_{1/2}$) for the isolated tissue experiments was 47 ± 5 R*, and the mean conditioning exposure used was 375 ± 37 R*/s. These intensity calculations are possibly on the high side, given some variability in positioning of the stimulus and the random orientation of the isolated retina outer segments. There was also a variable undershoot in some preparations that may have represented incomplete block of the slow Müller cell activity or residual bipolar cell activity (see Fig. 3). We performed isolated retina experiments in WT mice showing that a second flash of equivalent strength, delivered

during the undershoot, elicits an identical response, when compared with the first flash magnitude (1.00 ± 0.01 first flash, 1.02 ± 0.02 during undershoot; $n = 14$ trials in four retinas; $P > 0.3$). The presence of the undershoot may have been affected by how long the retina was exposed to 10 mM Ba^{2+} before starting perfusion of Locke's buffer. Saturating light intensities were determined empirically by stimulating with a 200-ms flash bright enough to saturate the cell response for at least 300 ms. The tyrosine kinase inhibitors Tyrphostin I-OMe AG538 (Sigma-Aldrich), Tyrphostin AG1024 (Enzo Life Sciences), and $HNMPA(AM)_3$ (Enzo Life Sciences) were each prepared in DMSO before being added to Locke's buffer for an experiment. Working solutions contained <1% DMSO. Final concentrations were chosen based on literature reports of the EC_{50} for each compound: Tyr538 at 1 µM lacks specificity for inhibiting the IGF1R and the IR (Blum et al., 2000); Tyr1024 at 250 nM is significantly more specific for IGF-1R than the IR (Párrizas et al., 1997); $HNMPA(AM)_3$ at 200 µM is specific for IR kinase inhibition (Gupta et al., 2012). The tyrosine phosphatase inhibitor sodium orthovanadate (Na_3VO_4; Sigma-Aldrich) stock was prepared in diH_2O and adjusted to pH 10.0 before being added to Locke's buffer for a final experimental solution concentration of 200 µM and pH of 7.4. Inhibitors were perfused onto the retina for at least 15 min before potentiation was tested. To monitor any changes introduced by the compounds, light responses were tested each minute during inhibitor exposure. The effects of orthovanadate and Tyrphostin 1024 did not appear to be reversible, as even 1 h of washout was not sufficient to restore AP. Light was delivered to the photoreceptors from a fiber-optic cable held in place above a glass coverslip. Light stimuli were controlled as in single cell experiments. Electrical responses were amplified (CP122W; Astro-med; DC 300 Hz) and digitized at 2 KHz (Real-Time PXI Computer; National Instruments). Light responses were collected for dim flashes up to rod saturating flashes to establish preparation stability. Isolated tissue responses were low-pass filtered post-hoc at 30 Hz, 8-pole Bessel.

Statistics

All p-values were calculated using a paired Student's *t* test using two-tailed assumptions.

RESULTS

Larger current amplitude after saturating light exposure

Suction electrode recordings were used to measure the response properties of single rod photoreceptors in three genotypes of mice (Table 1). Exposure to short-term (1–5 min) saturating light produced hypersensitivity in isolated WT mouse rods (Fig. 1). AP is demonstrated by responses recorded from a single mouse rod to test flashes of fixed intensity, presented in darkness, each
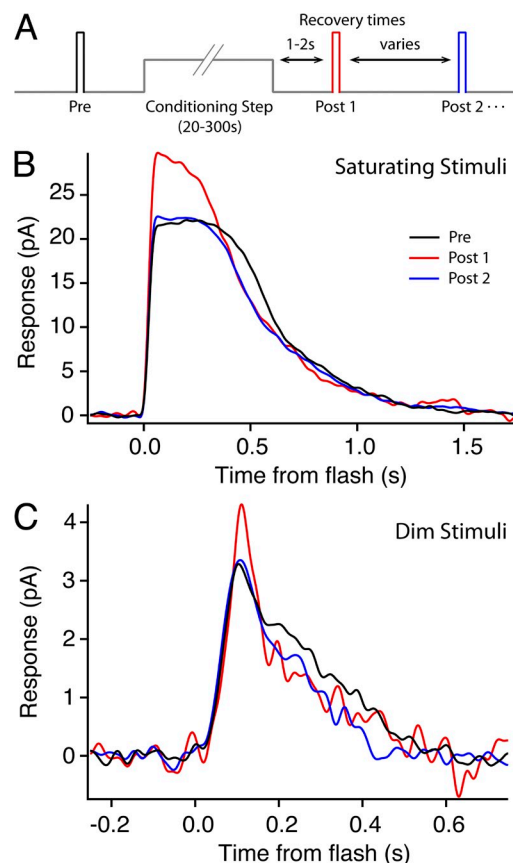

Figure 1. Photocurrents demonstrate AP after conditioning light exposure in isolated rods. (A) Schematic for all potentiation experiments. Identical test flashes were presented before and after a rod-saturating step of light. The colors of the test stimulus bars in A indicate the timing of the traces in B and C. (B) Representative saturating responses before (black, an average of three responses), 5 s after (red, single response), and 35 s after (blue, single response) the conditioning light (240 R*/s) was extinguished. R_{max} increased 36%. (C) In another cell, subsaturating responses recorded before (black, average of 10 responses), 5 s after (red, single response), and 15 s after (blue, single response) a 3-min conditioning light (200 R*/s). The peak amplitude of the response increased 30%.

producing 430 photoisomerizations (R*) before and after a conditioning step of light. Before the light step, the first test flash elicited a mean response of 21.7 pA, which represented saturation (Fig. 1 B, black trace).

TABLE 1
Single cell response parameters

Mouse line	R_{max}	$I_{1/2}$	I_t	$S_{(f)}$	τ_D
	pA	*R**	*ms*	*pA/R**	*ms*
WT (51)	12.6 ± 0.4	23.0 ± 1.0	292 ± 15	0.38 ± 0.03	172 ± 4
CaMΔ (20)	11.3 ± 0.9	21.0 ± 1.8	312 ± 26	0.31 ± 0.03	168 ± 7
$GCAP^{-/-}$ (15)	11.4 ± 1.5	13.0 ± 1.6	470 ± 35	1.2 ± 0.2	191 ± 7

Parameters tested for single cell recordings in WT, calmodulin-binding site deletion mice (CaMΔ), and GCAP1 and GCAP2 knockout mice ($GCAP^{-/-}$). R_{max} is the maximum dark-adapted circulating current. $I_{1/2}$ is the number of activated rhodopsin molecules sufficient to elicit a half-maximal response. I_t measures integration time of the rods to dim flashes. $S_{(f)}$ represents flash sensitivity in pA/activated rhodopsin. τ_D is a measure of the dominant time constant of recovery, measured at 75% of maximal response. All measures are mean ± 1 SEM.

Next, a 3-min conditioning light producing 250 R*/s was presented. Immediately after the conditioning light was extinguished, the test flash elicited a maximum response of 29.6 pA (Fig. 1 B, red trace). Subsequent test flashes showed that the enhanced photocurrent returned to its smaller, preadapted amplitude (Fig. 1 B, blue trace). In the 15 cells tested with 3-min conditioning exposures, the maximum photocurrent increased a mean of $31 \pm 2.7\%$ (Table 2), from 13.9 ± 1.2 to 18.4 ± 1.5 pA (P < 0.05). This light-dependent increase in outer segment photocurrent will be called AP. After conditioning stimuli, the photoresponses also recovered much faster, that is with shorter saturation periods than in the dark-adapted state. This adaptive acceleration was previously reported by Krispel et al. (2003), and we will show that it is a distinct and separate phenomenon from AP. Subsaturating response amplitudes were also enhanced after the conditioning light. In a dark-adapted rod, a dim test flash produced 19 R* and elicited a mean peak response of 3.32 pA (Fig. 1 C, black trace). After a 3-min conditioning exposure that activated 200 R*/s, the test flash evoked a peak response of 4.22 pA (Fig. 1 C, red trace), which returned to preadaptation levels after 15 s (Fig. 1 C, blue trace). In seven cells tested with dim flashes, after 3-min conditioning exposures, the mean AP was $29 \pm 4\%$, indicating that the increase in sensitivity is about the same magnitude across the working range of the cell.

To determine the threshold and integration time of the AP effect, we varied the conditioning exposure times from 20 s up to 5 min. AP was detectable with a 20-s conditioning stimulus ($8 \pm 1.9\%$) and grew to a peak of $31 \pm 2.7\%$ for 3-min exposures (Fig. 2 A). Exposure times <20 s may have produced small increases in circulating current, but such changes were difficult to detect. Conditioning exposures >3 min produced potentiation of <25% (Fig. 2 A). Fig. 2 B shows the time course of recovery to dark-adapted sensitivity. The conditioning stimulus ends at t = 0, and measureable potentiation is present as early as 2 s, peaking at ~5 s. The enhanced response amplitudes returned to preexposure (dark) levels with a time course well fit by a single exponential. The time constant of recovery (τ_{rec}) was 6.8 ± 0.7 s for 3-min conditioning exposures. The recovery time constant of AP was not significantly different for 30-, 60-, and 180-s conditioning stimuli, suggesting that the recovery mechanism is independent of the magnitude of the potentiation and the time over which it is developed (Fig. 2 B).

AP is present in isolated retina

To examine the adaptation in a population of photoreceptors unperturbed by suction electrodes, electroretinography was performed on isolated retinas. Using a pharmacological blockade (25 µM AP-4 and 10 mM aspartate) to prevent synaptic transmission from photoreceptors to ON-bipolar cells, the photoreceptor signal was studied in detail. In WT retinas, the photovoltage response to a rod-saturating test flash of fixed intensity increased from 180 ± 16 to 280 ± 22 µV after a 3-min conditioning light exposure ($n = 22$; P < 0.02), a mean of $38 \pm 2\%$, close to what was observed in single cells.

AP is eliminated by inhibiting phosphorylation pathways

Isolated retina ERGs were recorded to investigate the effects of blocking phosphorylation pathways on AP. IR kinase activity is capable of phosphorylating the CNG channel in a light-dependent manner, thus reducing the sensitivity of the channel for cGMP (Gupta et al., 2012). An opposing pathway, possibly mediated by the IGF-1R, promotes phosphatase activity and dephosphorylation of the channel (Savchenko et al., 2001). When a nonspecific inhibitor of both IGF-1R and IR kinase activity (Tyrphostin-I-OMe AG538) was applied, AP was eliminated (not depicted). To isolate the IR kinase activity, an IR-specific inhibitor was used (HNMPA(AM)$_3$). AP, measured in control conditions (Fig. 3 A, left), persisted in the presence of HNMPA(AM)$_3$ at 100 µM ($n = 3$; not depicted) and at 200 µM ($n = 3$; Fig. 3 A, right). These results confirm that the light-dependent phosphorylation of the channel by the IR is not involved in AP (see Discussion and Fig. 7). A specific inhibitor of the IGF-1R was used to isolate the IGF-1R pathway (Tyrphostin AG1024). Tyr1024 at 250 nM abolished AP in seven of seven WT retinas (e.g., Fig. 3 B). Instead of potentiation, there was a reduction in amplitude in the presence of Tyr1024 after the conditioning stimulus ($-24 \pm 6\%$; $n = 7$). The light-dependent

TABLE 2

AP measurements

Mouse line	R$_{max}$ pre	R$_{max}$ post	% Increase	τ_{rec}
	pA	*pA*		*s*
WT (15)	13.9 ± 1.2	18.4 ± 1.5	31 ± 3	6.8 ± 0.7
CaMΔ (16)	11.2 ± 0.9	17.7 ± 1.4	59 ± 4[a]	8.5 ± 0.8
GCAP$^{-/-}$ (13)	10.8 ± 1.1	17.8 ± 1.9	68 ± 8[a]	4.3 ± 0.9

AP elicited by a 3-min conditioning stimulus was calculated. R$_{max}$ pre represents dark-adapted mean amplitude before light exposure. R$_{max}$ post indicates the mean potentiated amplitude immediately after light exposure. The % increase indicates the mean increase in maximum current. τ_{rec} refers to the time constant of recovery of the potentiated amplitudes back to dark-adapted amplitudes. The conditioning stimulus intensity was selected to just saturate the rod in each experiment.

[a]Significant difference from WT (P < 0.001).

amplitude reduction caused by Tyr1024 in the bath was blocked when 250 nM Tyr1024 was combined with 200 µM HNMPA(AM)₃ (P < 0.01; Fig. 3 C), indicating that when both the IGF-1R and IR are blocked, the channel phosphorylation state is unaltered by light exposure. When activated by exogenous IGF-1, the IGF-1R promotes the dephosphorylation of tyrosine 498 of the CNG α subunit through an intermediate phosphatase, increasing the affinity of the channel for cGMP (Savchenko et al., 2001). To examine this downstream phosphatase activity, a broad-acting tyrosine phosphatase inhibitor was used (orthovanadate). AP could not be elicited in the presence of 200 µM orthovanadate ($n = 4$; e.g., Fig. 3 D). Collectively, results

Figure 2. The magnitude of AP is dependent on the duration of the conditioning light exposure. (A) Compared with precondition flash amplitude, represented as baseline (0% increase), potentiated amplitudes increased in magnitude with conditioning stimulus duration up to 3 min and declined with longer exposure times. The cell numbers for the various conditioning durations were 20 s, $n = 5$; 30 s, $n = 9$; 60 s, $n = 14$; 120 s, $n = 5$; 180 s, $n = 14$; 240 s, $n = 5$; and 300 s, $n = 2$. (B) Pooled data of amplitudes for all cells at three conditioning durations. Red circles indicate 180 s, $n = 14$; blue circles indicate 60 s, $n = 10$; green circles indicate 30 s, $n = 9$. The smooth trace in each graph is an exponential fit to the mean recovery data points: red line = 180-s exposure, $\tau_{rec} = 6.8$ s; blue line = 60-s exposure, $\tau_{rec} = 5.3$ s; green line = 30 s exposure, $\tau_{rec} = 5.6$ s. All responses were normalized to the preexposure (dark adapted) amplitude, and test flashes were presented every 2.5 s after light exposure. Error bars in all panels indicate ±1 SEM.

from these pharmacological manipulations suggest a pathway mediated by IGF-1R kinase activity as a probable mechanism for AP (see Fig. 7). In support of this model, exogenously applied IGF-1 (0.5 nM) enhanced the response amplitudes in isolated tissues (26%), and the presence of IGF-1 eliminated the AP ($n = 4$; not depicted).

Additional effects on the photoresponse after kinase and phosphatase inhibition

Each inhibitor also subtly affected the way the retinas responded to test stimuli in the absence of conditioning stimuli. Tyr1024 reduced the maximum response amplitude during recording by 15% (P < 0.05; $n = 5$) and tended to decelerate the recovery phase, whereas HNMPA(AM)₃ had the opposite effect and increased the overall amplitude of the response by 11% (P < 0.05; $n = 3$) and appeared to accelerate recovery rates. These results suggest that some basal rates of activation of the IR and IGF-1R pathways are present in the dark-adapted retina controlling channel phosphorylation in the absence of any conditioning light stimuli. Application of orthovanadate did not significantly alter the response amplitude, but it did dramatically accelerate the response recovery, possibly as the result of nonspecific inhibition of tyrosine phosphatases, such as protein tyrosine phosphatase-1B, which may regulate the PDE-γ subunit (Woodruff et al., 2014). In AP, saturating illumination appears to stimulate IGF-1R kinase activity, leading to CNG channel dephosphorylation and enhancing the rod photoreceptor's sensitivity to light, although the exact mechanism of action is unclear at this time.

Calmodulin interaction with CNG channels suppresses potentiation magnitude

Calmodulin influences the sensitivity of the CNG channel to cGMP, and thus it may potentially interact with the phosphorylation pathways described above. To explore the influence of the calmodulin–CNG channel interaction on AP, similar light exposure experiments were performed using a genetically modified mouse whose rods lack the calmodulin-binding site on the β subunit of the CNG channel. Removing the calmodulin-binding site almost doubled the AP amplitude for saturating test flashes, compared with that observed in WT rods (CaMΔ: 60 ± 4.1%, $n = 16$; WT: 31 ± 2.7%, $n = 15$; P < 0.001; Fig. 4 A and Table 2). The time constant of potentiation recovery was not significantly different between WT and the CaMΔ rods (CaMΔ: $\tau_{rec} = 8.5 ± 0.8$ s, $n = 14$; WT: $\tau_{rec} = 6.8 ± 0.7$ s, $n = 15$; P > 0.2; Fig. 4 B). Note that the CaMΔ rods showed earlier and larger increases in amplitude after conditioning stimuli; thus, the time to peak of AP was faster in the CaMΔ rods. These results imply that calmodulin works to temper AP after prolonged saturating light exposure because removing the calmodulin influence on the CNG channel results in larger current fluctuation and overshoot of the recovering photocurrent. The results from
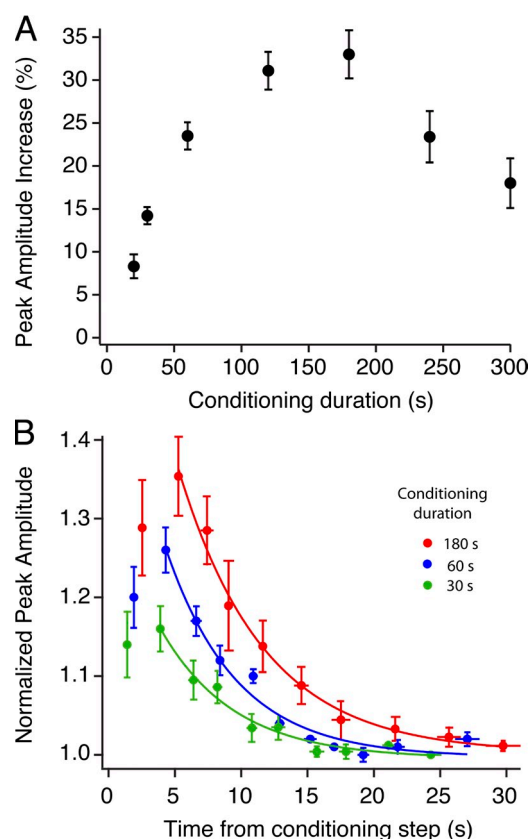
McKeown and Kraft   737

single cells were confirmed using isolated tissue ERG experiments; retinas from CaMΔ mice showed a significantly greater potentiation after 3-min saturating light exposures (CaMΔ: 64 ± 15% potentiation, n = 6; WT: 35 ± 3% potentiation, n = 19; P < 0.001). As in the WT retinas, application of 250 nM Tyr1024 eliminated AP in CaMΔ tissues (n = 7; Fig. 4 C). The responses after conditioning exposure were consistently smaller than preexposure levels before returning to baseline ($-30 ± 7\%$; n = 7), a reduction which was not significantly different from that seen in WT (P > 0.5).

Extended potentiation lifetime with lowered Mg

GCAPs are key components in terminating the rod light response, and we studied their role in AP. To examine the effects Mg^{2+} concentration may have on the intracellular signaling pathways involving GCAPs and guanylate cyclase, we performed single cell recordings in Locke's buffer that contained half the standard concentration of Mg^{2+}, reduced from 2.4 to 1.2 mM. To validate the effects of the reduced Mg^{2+}, we also measured the dominant

time constant of recovery (τ_D), which is a metric of the photoresponse recovery to saturating flashes (Pepperberg et al., 1992). τ_D has been shown to be sensitive to extracellular Mg^{2+}, increasing from τ_D = 173 to 376 ms when the Mg^{2+} concentration is reduced from 2.4 to 1.2 mM (Azevedo and Rieke, 2011). Our recordings from rods exposed to lower Mg^{2+} showed a similar increase in τ_D (171 to 291 ms). Interestingly, AP was still generated in the presence of lowered Mg^{2+}, and it had a similar magnitude (Fig. 5 A). However, the recovery to dark baseline was slowed by nearly a factor of two compared with cells bathed in standard Locke's buffer (low Mg^{2+}: τ_{rec} = 13.3 ± 1.2 s, n = 8; control Mg^{2+}: τ_{rec} = 6.8 ± 0.7 s, n = 15; P < 0.005; Fig. 5 B). These results suggest that the origins of the potentiation are unaffected by lowered Mg^{2+} concentration, but the mechanisms that govern recovery are Mg^{2+} sensitive.

Given the GCAP dependence on Mg^{2+} concentration, experiments were performed on rods lacking GCAP proteins (GCAP$^{-/-}$ mice). AP was present in GCAP$^{-/-}$ rods and was more than double the magnitude seen in WT
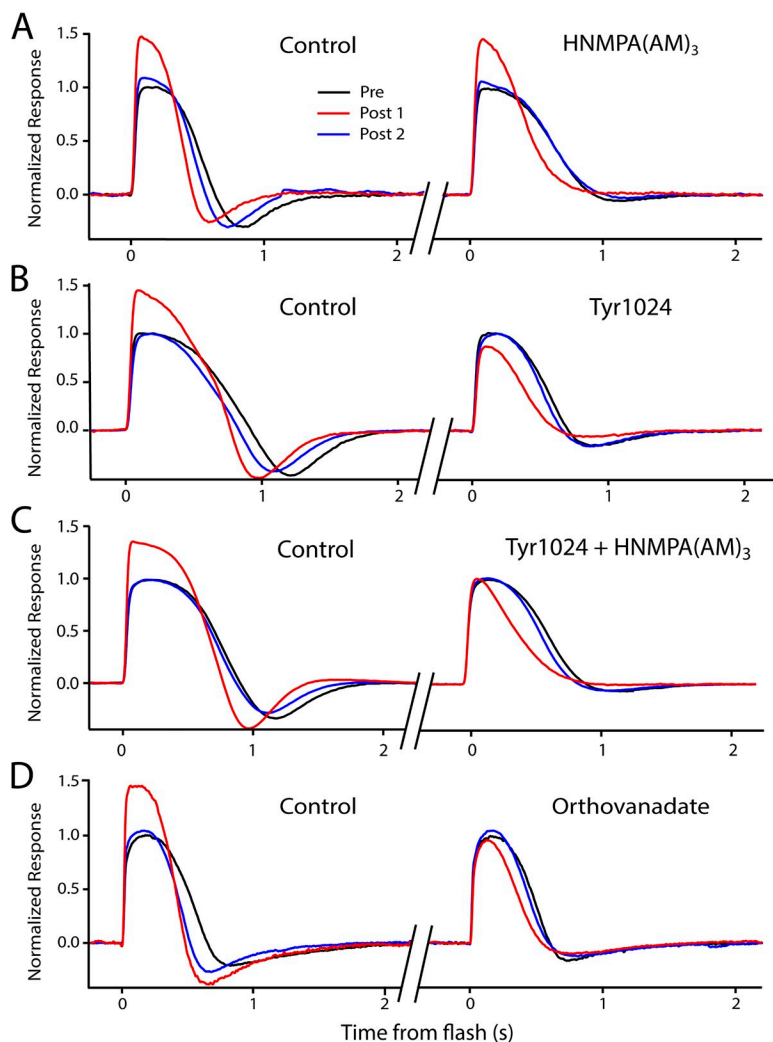

Figure 3. Kinase and phosphatase inhibitors influence light-induced potentiation in isolated retina recordings. All figures show a dark-adapted response (black trace, average of three to five responses), a response recorded 3–5 s after 3-min saturating light (red trace, single response), and a third response, recorded 20–30 s later, representing recovery (blue trace, single response). (A–D) Each panel shows two potentiation experiments on a single retina before (left) and after (right) the application of the indicated drug or drugs. (A) Potentiation is present in control solution (left), showing a 46% increase in peak amplitude before application of HNMPA(AM)₃, a specific blocker of IR kinase activity. The presence of 200 µM HNMPA(AM)₃ did not affect the potentiation (right), as the potentiation (red trace) persists in the presence of the inhibitor. (B) Potentiation is present in control solution (left), showing a 36% increase in amplitude before application of Tyr1024, a specific blocker of IGF-1R kinase activity. The presence of 250 nM Tyr1024 eliminated the potentiation (right) after a conditioning light; in fact, there was a decrease in amplitude that recovered with time (blue trace). (C) Application of both 250 nM Tyr1024 and 200 µM HNMPA(AM)₃ eliminates potentiation and the amplitude reduction after light exposure seen with Try1024 alone. (D) Potentiation is present in control solution (left), showing a 44% increase in amplitude before application of orthovanadate, a broad-acting inhibitor of tyrosine phosphatases. The presence of 200 µM orthovanadate eliminates the potentiation (right).
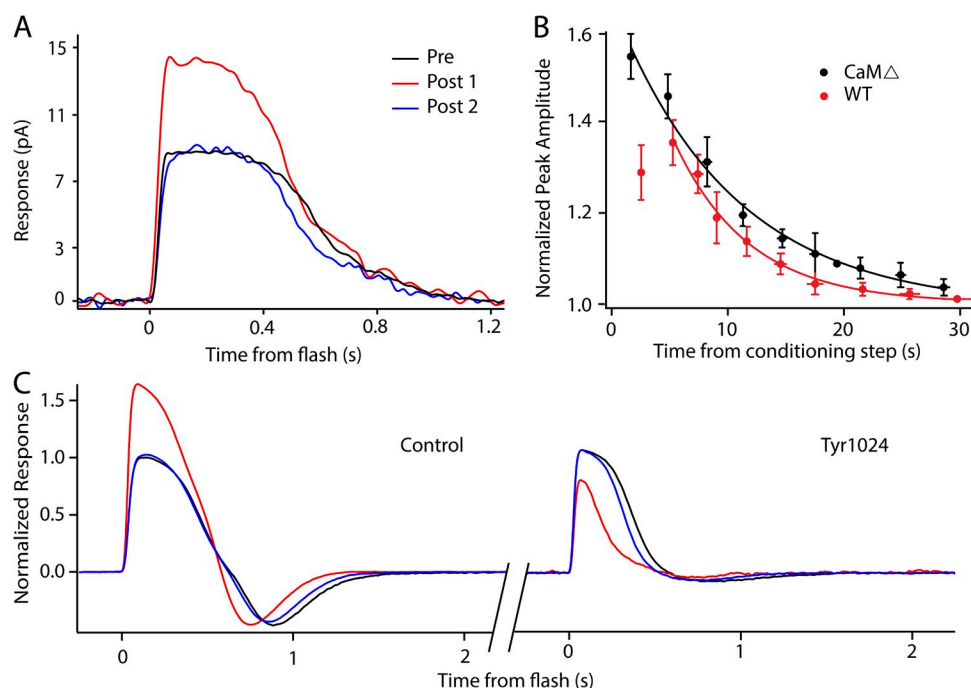
Figure 4. AP is larger and appears sooner in CaMΔ rods. (A) A representative trace from a single CaMΔ cell exhibiting potentiation. The response increased 60%, from 9.2 pA in darkness (black trace) to 14.7 pA (red trace) after a 3-min conditioning exposure. The response recovered to baseline (blue trace) with a time constant of 7.2 s. (B) Response amplitudes of AP after 3-min conditioning stimulus (off at t = 0). Pooled data from WT (red circles; $n = 15$) and CaMΔ rods (black circles; $n = 14$) demonstrate an overall increase in amplitude and a faster time to peak of the adaptation in CaMΔ rods. Traces represent exponential fits to ensemble data for WT (red line), $\tau_{rec} = 6.8 \pm 0.7$ s; and CaMΔ (black line), $\tau_{rec} = 8.5 \pm 0.8$ s. Error bars indicate ±1 SEM. (C) A larger potentiation was also present in isolated CaMΔ retina ERGs, increasing 64% from 175 µV (black trace) to 287 µV (red trace) after a 3-min conditioning exposure before recovering to baseline (blue trace). Potentiation in the same retina was blocked with application of 250 nM Tyr1024 (right). The response amplitude was reduced after the conditioning light exposure (red trace), similar to the results in WT, and then recovered to baseline amplitude (blue trace).

rods (GCAP$^{-/-}$: 68 ± 8% potentiation, $n = 13$; WT: 31 ± 2.7% potentiation, $n = 15$; P < 0.001; Fig. 6 A and Table 2). GCAP$^{-/-}$ rods appeared to recover slightly faster when compared with WT rods, but the rates were not significantly different (GCAP$^{-/-}$: $\tau_{rec} = 6.0 \pm 1.0$ s, $n = 12$; WT: $\tau_{rec} = 6.8 \pm 0.7$ s, $n = 14$; P > 0.15). Note also that the acceleration of the light response seen in WT and CaMΔ rods is absent in the GCAP$^{-/-}$ rods (Fig. 6 B). Low Mg did not affect the time course of recovery in GCAP$^{-/-}$ rods (GCAP$^{-/-}$: $\tau_{rec} = 6.0 \pm 1.0$ s, $n = 12$; GCAP$^{-/-}$ low Mg^{2+}: 4.4 ± 0.4 s, $n = 6$; P > 0.25; Fig. 6 C). This finding indicates separate mechanisms for the adaptive acceleration of the

response reported by Krispel et al. (2003) and the AP reported here. We also rule out GCAP–guanylate cyclase feedback as the origin of AP.

DISCUSSION

In the current accounts of light adaptation, rod responses get smaller in magnitude and recover faster (Tamura et al., 1991; Woodruff et al., 2008). Upon cessation of the light, the rate at which sensitivity recovers to dark-adapted levels is largely dependent on the amount of rhodopsin bleached by the adapting illumination (Kang Derwent
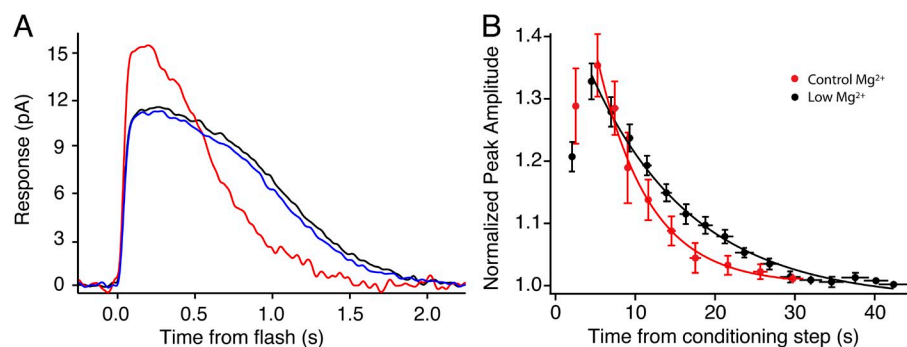

Figure 5. Lowering extracellular Mg^{2+} prolongs the period of AP in isolated rods. (A) A representative trace exhibiting potentiation in low extracellular Mg^{2+}. The response increased 34%, from 11.6 pA in darkness (black trace) to 15.6 pA (red trace) after a 3-min conditioning exposure. The response recovered to baseline (blue trace) with a time constant of 11.9 s. (B) Traces represent an exponential fit to the recovery of AP after a 3-min conditioning stimulus (off at t = 0). Results were normalized to the dark-adapted amplitude. Recovery in standard, 2.4 mM [Mg^{2+}]$_{ext}$ (red line), $\tau_{rec} = 6.8 \pm 0.7$ s, $n = 15$; recovery in low, 1.2 mM [Mg^{2+}]$_{ext}$ (black line) $\tau_{rec} = 13.3 \pm 1.2$ s. Error bars indicate ±1 SEM.

McKeown and Kraft 739

et al., 2002). Here we present a form of adaptation where immediately after rod-saturating illumination the rod response is larger than what was observed in darkness just minutes earlier. This finding clearly deviates from the existing models of light and dark adaptation. AP was found for saturating and linear range responses, indicating that the rods have heightened sensitivity across their working range. The potentiation builds as conditioning exposure time increases and likely reflects some underlying
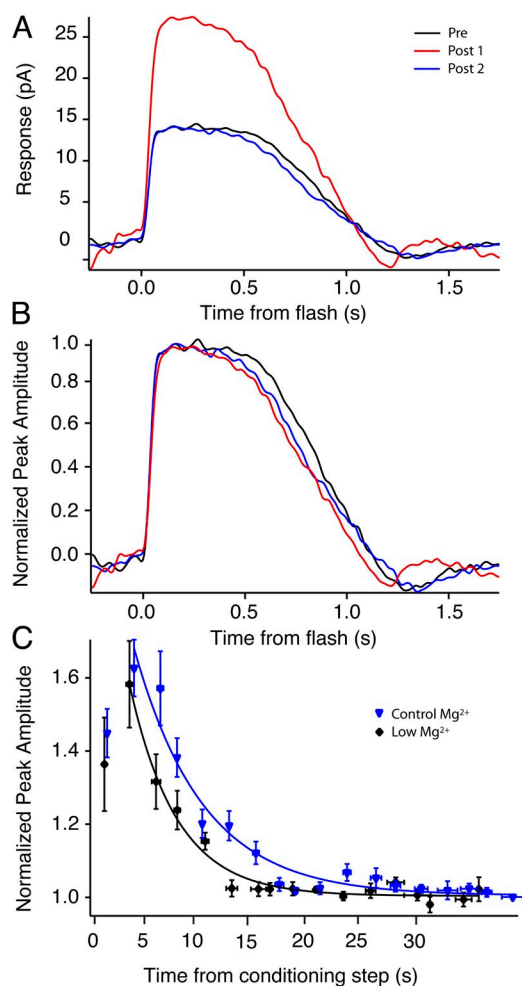

Figure 6. AP is present in $GCAP^{-/-}$ mice and is unaffected by extracellular Mg^{2+} concentration. (A) Representative potentiation in a $GCAP^{-/-}$ rod, showing an increase of 92%, from 14.2 pA in darkness (black trace) to 27.3 pA (red trace) after a 3-min conditioning exposure. The response recovered to baseline (blue trace) with a time constant of 4.3 s. (B) Normalizing the responses in A shows no acceleration (reduction of the saturation period) after the conditioning exposure, contrary to what is seen in WT and CaMΔ mice. (C) Pooled data of recovering amplitudes for $GCAP^{-/-}$ cells in normal and low extracellular Mg^{2+}. The smooth trace in each graph is an exponential fit to the mean recovery data points. Time constants of recovery were not significantly different between conditions: normal Mg^{2+} (blue line), $\tau_{rec} = 5.97 \pm 0.99$ s, $n = 12$; low Mg^{2+} (black line), $\tau_{rec} = 4.40 \pm 0.37$ s, $n = 6$. All responses were normalized to the preexposure (dark adapted) amplitude and test flashes. Error bars indicate ±1 SEM.

mechanism of adaptation that is maximally evoked at 3 min and diminishes thereafter. The increased sensitivity of AP is extremely robust, unfailingly occurring in 86 single cell recordings and in 34 isolated retina recordings from multiple lines of mice. A limited number of recordings indicate that AP is also present in primate rod photoreceptors of the *Macaca nemestrina*, suggesting that this phenomenon is not limited to nocturnal animals (unpublished data). In both mouse and primate, the adaptation was present in cells embedded within the photoreceptor layer and in cells completely isolated from any surrounding photoreceptors, arguing against any feedback from other cells as a cause and suggesting the mechanism of adaptation is likely restricted to the rod outer segment.

Isolated retina ERG recordings revealed the effects of kinase and phosphatase inhibitors on the photoreceptor response (Fig. 7). Phosphorylation of the CNG channel occurs on two tyrosine residues, and phosphorylation has been shown to decrease channel sensitivity for cGMP, which in turn depresses photoresponse amplitude (Gordon et al., 1992; Molokanova et al., 1999). IGF-1 is released by the RPE, and can be sequestered in the interphotoreceptor matrix by IGF-1–binding proteins (Waldbillig et al., 1991). Indeed, application of exogenous IGF-1 has been shown to stimulate a phosphatase pathway that results in dephosphorylation of the channel and larger response amplitudes (Savchenko et al., 2001). Given the availability of IGF-1 in the interphotoreceptor matrix and the effects of IGF-1 on the photoresponse, it is appealing to propose that the photoresponse may somehow liberate extracellular IGF-1, which then modulates channel sensitivity. An opposing pathway has been described, wherein light-activated rhodopsin can stimulate the IR to phosphorylate the CNG channel (Rajala and Anderson, 2003; Gupta et al., 2012). We have shown that inhibition of the IGF-1R and inhibition of tyrosine phosphatases blocked AP, whereas inhibition of the IR alone had no effect. These results suggest that the phosphorylation of the CNG channel plays a physiological role in light and dark adaptation and is determined by the length and intensity of light exposure.

Each inhibitor also affected the way the retinas responded to constant stimuli in the absence of conditioning light. Application of Tyr1024, the IGF-1R–specific inhibitor, significantly reduced the maximum response amplitude, independent of light exposure. Also, Tyr1024 application reduced the response below baseline, where there should have been potentiation. This effect was blocked by coapplication of HNMPA(AM)₃, indicating that the IGF-1R and IR kinase activity are in opposition. Additionally, application of the IR inhibitor HNMPA(AM)₃ increased the overall amplitude of the response, probably by allowing the IGF-1R branch of the pathway to dominate and reduce channel phosphorylation. Thus, the basal IR and IGF-1R activities are influencing cell sensitivity

in darkness. Indeed, the basal activity of the IR kinase is higher in retina than in liver and is relatively constant between freely fed and fasted rats (Reiter et al., 2003). We show that the magnitude of AP declines with conditioning durations of >3 min, possibly indicating a shift in the controlling influence from the IGF-1 to the IR pathway.

The results from the CaMΔ and GCAP$^{-/-}$ mice further refined the complex picture of potentiation. Ca^{2+}-calmodulin and GCAPs are part of cation-dependent feedback mechanisms, and changing the extracellular concentration of cations can affect response kinetics (Dizhoor et al., 2010; Azevedo and Rieke, 2011). The ratio of Mg^{2+} to Ca^{2+} is a critical factor in determining GCAP-mediated recovery kinetics of the cellular response to a saturating stimulus. The channel phosphorylation changes that occur in response to periods of saturating illumination in our experiments are likely to occur more slowly than the rapid Ca-dependent GCAPs feedback pathway acting through guanylate cyclase.
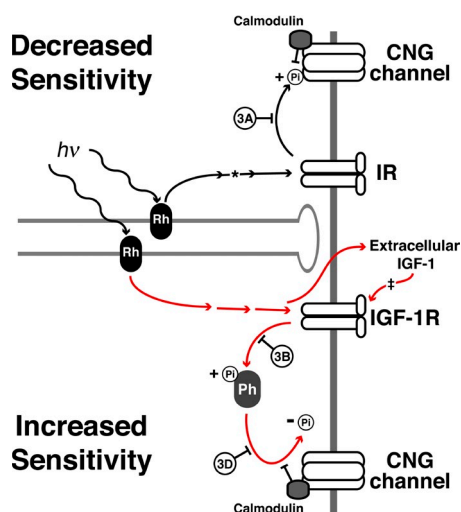

Figure 7. A model representing a possible mechanism of AP. The established pathway between rhodopsin (Rh), the IR, and the CNG channel is likely not involved in AP, as blocking IR kinase activity failed to abolish the adaptation (top path, inhibition experiment in Fig. 3 A). The asterisk represents work by Rajala and Anderson (2003), Rajala et al. (2007), Gupta et al. (2012), and Woodruff et al. (2014). The red lines represent the proposed pathways involved in increasing sensitivity. Here, incident light activates the IGF-1R, possibly through a pathway similar to the IR or through a separate pathway involving extracellular IGF-1 release. The IGF-1R then activates a phosphatase (Ph) that dephosphorylates the CNG channel, increasing channel sensitivity for cGMP. Blocking the activity of the IGF-1R or the tyrosine phosphatase eliminates AP (bottom path, inhibition experiments in Fig. 3, B and D). The ‡ represents work by Savchenko et al. (2001), in which the effects of externally applied IGF-1 were demonstrated. Calmodulin is present in both the top and bottom panels, indicating a potential role for interference of kinase or phosphatase activity as proposed by Krajewski et al. (2003) and supported by Fig. 4 D.

Indeed, GCAP$^{-/-}$ mice exhibited larger changes in circulating current after light steps, similar to the undershoot of current previously reported (see Fig. 5 in Chen et al. [2010]). Our findings reveal the importance of GCAPs in not only determining response recovery to single flashes, but in determining the magnitude of light responses after conditioning light exposure. Any disruption of the Mg^{2+} and Ca^{2+} homeostasis in the extracellular space likely has a significant impact on cellular sensitivity and function.

Light-dependent changes in Ca concentration strongly influence cell sensitivity. During sustained illumination, outer-segment Ca levels fall to 20 nM or less, below the binding K$_m$ for calmodulin (49 nM Ca^{2+}; Nakatani et al., 1995; Matthews and Fain, 2003). Calmodulin then dissociates from the CNG channels, increasing channel sensitivity to cGMP by at least threefold (Bauer, 1996). We found that deletion of the calmodulin-binding site on the channel resulted in larger AP than WT controls, and the rise of the potentiation was much faster than in WT rods. Thus, calmodulin plays an important role in reducing channel sensitivity and counteracting the rapid production of cGMP by guanylate cyclase. Calmodulin binding to the CNG channels is also dependent on the channel phosphorylation state, and both calmodulin binding and channel phosphorylation reduce channel sensitivity (Krajewski et al., 2003). Perhaps when Ca^{2+} falls and calmodulin dissociates, the channels are more accessible to tyrosine kinases and phosphatases. Indeed, in the absence of the calmodulin-binding site, the channels were more susceptible to cycling of the phosphorylation state (Fig. 4). Calmodulin appears to play a more substantial role in adaptation than previously suggested (Chen et al., 2010) by limiting a fast component of the phosphorylation-dependent sensitivity of the channel after light exposure.

All of these results are consistent with a model in which light-dependent activation of the IGF-1R increases the sensitivity of the rod photoreceptor (Fig. 7). Hypersensitivity in darkness after a rod-saturating illumination may provide an evolutionarily advantage. Enhancing the signal transmitted from individual rods to bipolar cells could improve perceptual sensitivity under scotopic or mesopic conditions.

REFERENCES

Azevedo, A.W., and F. Rieke. 2011. Experimental protocols alter phototransduction: the implications for retinal processing at visual threshold. *J. Neurosci.* 31:3670–3682. http://dx.doi.org/10.1523/JNEUROSCI.4750-10.2011

Bauer, P.J. 1996. Cyclic GMP-gated channels of bovine rod photoreceptors: affinity, density and stoichiometry of Ca^{2+}–calmodulin binding sites. *J. Physiol.* 494:675–685.

Baylor, D.A., T.D. Lamb, and K.-W. Yau. 1979. Responses of retinal rods to single photons. *J. Physiol.* 288:613–634.

Blum, G., A. Gazit, and A. Levitzki. 2000. Substrate competitive inhibitors of IGF-1 receptor kinase. *Biochemistry.* 39:15705–15712. http://dx.doi.org/10.1021/bi001516y

Breton, M.E., A.W. Schueller, T.D. Lamb, and E.N. Pugh Jr. 1994. Analysis of ERG a-wave amplification and kinetics in terms of the G-protein cascade of phototransduction. *Invest. Ophthalmol. Vis. Sci.* 35:295–309.

Burns, M.E., A. Mendez, J. Chen, and D.A. Baylor. 2002. Dynamics of cyclic GMP synthesis in retinal rods. *Neuron.* 36:81–91. http://dx.doi.org/10.1016/S0896-6273(02)00911-X

Chen, C.K., M.E. Burns, W. He, T.G. Wensel, D.A. Baylor, and M.I. Simon. 2000. Slowed recovery of rod photoresponse in mice lacking the GTPase accelerating protein RGS9-1. *Nature.* 403:557–560. http://dx.doi.org/10.1038/35000601

Chen, J., M.L. Woodruff, T. Wang, F.A. Concepcion, D. Tranchina, and G.L. Fain. 2010. Channel modulation and the mechanism of light adaptation in mouse rods. *J. Neurosci.* 30:16232–16240. http://dx.doi.org/10.1523/JNEUROSCI.2868-10.2010

Dizhoor, A.M., E.V. Olshevskaya, and I.V. Peshenko. 2010. Mg^{2+}/Ca^{2+} cation binding cycle of guanylyl cyclase activating proteins (GCAPs): role in regulation of photoreceptor guanylyl cyclase. *Mol. Cell. Biochem.* 334:117–124. http://dx.doi.org/10.1007/s11010-009-0328-6

Gal, A., U. Orth, W. Baehr, E. Schwinger, and T. Rosenberg. 1994. Heterozygous missense mutation in the rod cGMP phosphodiesterase β-subunit gene in autosomal dominant stationary night blindness. *Nat. Genet.* 7:64–68. http://dx.doi.org/10.1038/ng0594-64

Gordon, S.E., D.L. Brautigan, and A.L. Zimmerman. 1992. Protein phosphatases modulate the apparent agonist affinity of the light-regulated ion channel in retinal rods. *Neuron.* 9:739–748. http://dx.doi.org/10.1016/0896-6273(92)90036-D

Gupta, V.K., A. Rajala, and R.V. Rajala. 2012. Insulin receptor regulates photoreceptor CNG channel activity. *Am. J. Physiol. Endocrinol. Metab.* 303:E1363–E1372. http://dx.doi.org/10.1152/ajpendo.00199.2012

Jiang, L., and W. Baehr. 2010. GCAP1 mutations associated with autosomal dominant cone dystrophy. *Adv. Exp. Med. Biol.* 664:273–282. http://dx.doi.org/10.1007/978-1-4419-1399-9_31

Kang Derwent, J.J., N.M. Qtaishat, and D.R. Pepperberg. 2002. Excitation and desensitization of mouse rod photoreceptors in vivo following bright adapting light. *J. Physiol.* 541:201–218. http://dx.doi.org/10.1113/jphysiol.2001.013227

Karwoski, C.J., H.K. Lu, and E.A. Newman. 1989. Spatial buffering of light-evoked potassium increases by retinal Müller (glial) cells. *Science.* 244:578–580. http://dx.doi.org/10.1126/science.2785716

Krajewski, J.L., C.W. Luetje, and R.H. Kramer. 2003. Tyrosine phosphorylation of rod cyclic nucleotide-gated channels switches off Ca^{2+}/calmodulin inhibition. *J. Neurosci.* 23:10100–10106.

Krispel, C.M., C.K. Chen, M.I. Simon, and M.E. Burns. 2003. Novel form of adaptation in mouse retinal rods speeds recovery of phototransduction. *J. Gen. Physiol.* 122:703–712. http://dx.doi.org/10.1085/jgp.200308938

Krispel, C.M., D. Chen, N. Melling, Y.J. Chen, K.A. Martemyanov, N. Quillinan, V.Y. Arshavsky, T.G. Wensel, C.K. Chen, and M.E. Burns.

2006. RGS expression rate-limits recovery of rod photoresponses. *Neuron.* 51:409–416. http://dx.doi.org/10.1016/j.neuron.2006.07.010

Lyubarsky, A.L., L.L. Daniele, and E.N. Pugh Jr. 2004. From candelas to photoisomerizations in the mouse eye by rhodopsin bleaching in situ and the light-rearing dependence of the major components of the mouse ERG. *Vision Res.* 44:3235–3251. http://dx.doi.org/10.1016/j.visres.2004.09.019

Matthews, H.R., and G.L. Fain. 2003. The effect of light on outer segment calcium in salamander rods. *J. Physiol.* 552:763–776. http://dx.doi.org/10.1113/jphysiol.2003.050724

Mendez, A., M.E. Burns, I. Sokal, A.M. Dizhoor, W. Baehr, K. Palczewski, D.A. Baylor, and J. Chen. 2001. Role of guanylate cyclase-activating proteins (GCAPs) in setting the flash sensitivity of rod photoreceptors. *Proc. Natl. Acad. Sci. USA.* 98:9948–9953. http://dx.doi.org/10.1073/pnas.171308998

Molokanova, E., B. Trivedi, A. Savchenko, and R.H. Kramer. 1997. Modulation of rod photoreceptor cyclic nucleotide-gated channels by tyrosine phosphorylation. *J. Neurosci.* 17:9068–9076.

Molokanova, E., F. Maddox, C.W. Luetje, and R.H. Kramer. 1999. Activity-dependent modulation of rod photoreceptor cyclic nucleotide-gated channels mediated by phosphorylation of a specific tyrosine residue. *J. Neurosci.* 19:4786–4795.

Naeem, M.A., V.R. Chavali, S. Ali, M. Iqbal, S. Riazuddin, S.N. Khan, T. Husnain, P.A. Sieving, R. Ayyagari, S. Riazuddin, et al. 2012. GNAT1 associated with autosomal recessive congenital stationary night blindness. *Invest. Ophthalmol. Vis. Sci.* 53:1353–1361. http://dx.doi.org/10.1167/iovs.11-8026

Nakatani, K., Y. Koutalos, and K.-W. Yau. 1995. Ca^{2+} modulation of the cGMP-gated channel of bullfrog retinal rod photoreceptors. *J. Physiol.* 484:69–76.

Párrizas, M., A. Gazit, A. Levitzki, E. Wertheimer, and D. LeRoith. 1997. Specific inhibition of insulin-like growth factor-1 and insulin receptor tyrosine kinase activity and biological function by tyrphostins. *Endocrinology.* 138:1427–1433. http://dx.doi.org/10.1210/endo.138.4.5092

Pepperberg, D.R., M.C. Cornwall, M. Kahlert, K.P. Hofmann, J. Jin, G.J. Jones, and H. Ripps. 1992. Light-dependent delay in the falling phase of the retinal rod photoresponse. *Vis. Neurosci.* 8:9–18. http://dx.doi.org/10.1017/S0952523800006441

Rajala, A., R.E. Anderson, J.X. Ma, J. Lem, M.R. Al-Ubaidi, and R.V. Rajala. 2007. G-protein-coupled receptor rhodopsin regulates the phosphorylation of retinal insulin receptor. *J. Biol. Chem.* 282:9865–9873. http://dx.doi.org/10.1074/jbc.M608845200

Rajala, R.V., and R.E. Anderson. 2003. Light regulation of the insulin receptor in the retina. *Mol. Neurobiol.* 28:123–138. http://dx.doi.org/10.1385/MN:28:2:123

Reiter, C.E., L. Sandirasegarane, E.B. Wolpert, M. Klinger, I.A. Simpson, A.J. Barber, D.A. Antonetti, M. Kester, and T.W. Gardner. 2003. Characterization of insulin signaling in rat retina in vivo and ex vivo. *Am. J. Physiol. Endocrinol. Metab.* 285:E763–E774.

Savchenko, A., T.W. Kraft, E. Molokanova, and R.H. Kramer. 2001. Growth factors regulate phototransduction in retinal rods by modulating cyclic nucleotide-gated channels through dephosphorylation of a specific tyrosine residue. *Proc. Natl. Acad. Sci. USA.* 98:5880–5885. http://dx.doi.org/10.1073/pnas.101524998

Tamura, T., K. Nakatani, and K.-W. Yau. 1991. Calcium feedback and sensitivity regulation in primate rods. *J. Gen. Physiol.* 98:95–130. http://dx.doi.org/10.1085/jgp.98.1.95

Waldbillig, R.J., R.T. Fletcher, G.J. Chader, S. Rajagopalan, M. Rodrigues, and D. LeRoith. 1987. Retinal insulin receptors. 2. Characterization and insulin-induced tyrosine kinase activity in bovine retinal rod outer segments. *Exp. Eye Res.* 45:837–844. http://dx.doi.org/10.1016/S0014-4835(87)80100-8

Waldbillig, R.J., B.A. Pfeffer, T.J. Schoen, A.A. Adler, Z. Shen-Orr, L. Scavo, D. LeRoith, and G.J. Chader. 1991. Evidence for an insulin-like growth factor autocrine-paracrine system in the retinal photoreceptor-pigment epithelial cell complex. *J. Neurochem.* 57:1522–1533. http://dx.doi.org/10.1111/j.1471-4159.1991.tb06347.x

Woodruff, M.L., K.M. Janisch, I.V. Peshenko, A.M. Dizhoor, S.H. Tsang, and G.L. Fain. 2008. Modulation of phosphodiesterase6 turnoff during background illumination in mouse rod photoreceptors.

J. Neurosci. 28:2064–2074. http://dx.doi.org/10.1523/JNEUROSCI.2973-07.2008

Woodruff, M.L., A. Rajala, G.L. Fain, and R.V. Rajala. 2014. Modulation of mouse rod photoreceptor responses by Grb14 protein. *J. Biol. Chem.* 289:358–364. http://dx.doi.org/10.1074/jbc.M113.517045

Zick, Y., A.M. Spiegel, and R. Sagi-Eisenberg. 1987. Insulin-like growth factor I receptors in retinal rod outer segments. *J. Biol. Chem.* 262:10259–10264.